Standing wave in evaporating meniscus detected by infrared thermography

Citation for published version:
Buffone, C, Sefiane, K, Minetti, C & Mamalis, D 2015, 'Standing wave in evaporating meniscus detected by infrared thermography', *Applied Physics Letters*, vol. 107, no. 4, 041606. https://doi.org/10.1063/1.4927744

Digital Object Identifier (DOI):
10.1063/1.4927744

Link:
Link to publication record in Edinburgh Research Explorer

Document Version:
Peer reviewed version

Published In:
Applied Physics Letters

Standing wave in evaporating meniscus from a capillary tube detected by InfraRed thermography

Cosimo Buffone[1*], Khellil Sefiane[2,3], Christophe Minetti[1], Dimitrios Mamalis[2]

[1] Microgravity Research Centre, Université libre de Bruxelles, Avenue F. Roosevelt 50, 1050 Bruxelles, Belgium

[2] Institute for Materials and Processes, School of Engineering, The University of Edinburgh, EH9 3JL, Edinburgh, United Kingdom

[3] International Institute for Carbon-Neutral Energy Research (I2CNER)

Kyushu University, 744 Motooka, Nishi-ku, Fukuoka, 819-0395, Japan

Abstract

A standing wave has been detected in the evaporating meniscus formed on an organic liquid (acetone) inside a horizontally positioned capillary tube of 1 mm internal diameter. The standing wave is believed to originate from the interaction between surface tension and gravitational forces. We found that the standing wave ensues only at the upper part of the meniscus interface where gravity and surface tension act in the opposite direction. This experimental observation is similar to standing waves observed in floating zones in microgravity but different from travelling waves reported recently in volatile drops; in both cases the waves are produced by temperature differences along a liquid-vapour interface. By employing InfraRed thermography we recorded the temperature distribution of the meniscus interface and we found that the first characteristic frequency of the standing wave is around 0.3 Hz.

INTRODUCTION

Surface-tension-dominated phenomena are ubiquitous; they are found in numerous industrial applications from oil extraction to combustion, drug preparation, boiling, evaporation and condensation, crystal growth, and spreading of drops. Surface tension is responsible for defining the interface at the micro scale as demonstrated by Levich and Krylov [1]. The role of surface tension was first recognised by Pearson [2] in 1958, while the Marangoni number was first introduced in 1960 by Scriven and Sternling [3]. In the present study we examine a capillary tube with an internal diameter of 1 mm and use acetone as the evaporating liquid which leads to a capillary length of less than 2 mm. Therefore, we expect that thermo-capillary forces will be dominant. Nevertheless, Buffone *et al.* [4] reported significant distortion of the Marangoni cells because of the gravitational forces in the diametrical vertical section of the horizontally positioned tube. Buffone *et al.* [5] also reported important oscillations in the Marangoni vortex as well as in the meniscus interface.

* Corresponding author: Tel. 0032 2650 3029, Fax. 0032 2650 3126, Email cbuffone@ulb.ac.be

This suggested the presence of hydrothermal waves, such as those found in shallow liquid layers heated from the side [6-10] or in the more recently and intensively researched subject of sessile drops [11] or even standing waves found in liquid bridges [12].

RESULTS AND DISCUSSION

This letter reports a study of self-induced thermocapillary convection in the liquid phase of an evaporative meniscus of acetone inside a 1 mm internal diameter borosilicate tube positioned horizontally. Acetone evaporates at the tube mouth in still air at ambient conditions where no external heating is provided to the system. The evaporation rate along the curved meniscus interface is not uniform, being larger at the meniscus wedge than in the middle (Buffone and Sefiane [13]) and creates differences in temperature which in turn generate gradients of surface tension that is the driving mechanism for the convection observed. Along the horizontal optical sections of the tube, the surface tension is symmetrical; whereas along the vertical optical sections there is a competition between surface tension and gravity which produces a non-symmetrical driving force. Figure 1 shows the Particle Image Velocimetry of the liquid-side of the meniscus for a horizontal (left picture) and vertical (right picture) optical section of the capillary tube; clearly two counter-rotating vortex sections are present in the horizontal section, whereas a single vortex is present in the vertical section . Therefore, the Marangoni vortex has a distorted three-dimensional toroidal shape. The flow structures shown in Figure 1 oscillate in time as reported in Buffone et al. [4] and Buffone et al. [5], having a characteristic frequency depending mainly on tube size and liquid used.

Figure 1. Typical PIV analysis: (left) horizontal diametrical section of the capillary tube; (right) vertical diametrical section of the capillary tube. Vector **g** in the right picture is the gravitational acceleration. "Reproduced with permission from Buffone et al. Phys. Fluids 17, 052104; doi: 10.1063/1.1901688. Copyright 2005, AIP Publishing LLC."

Figure 2 shows InfraRed (IR) temperature measurements of the meniscus interface at the tube mouth at four different times. The tubes' external and internal walls are indicated with white circles. The dashed line shown on frames two and three of Figure 2 (obtained using a classical segmentation tool) is a qualitative delimitation of the region of interest for the standing wave. The IR camera used in this study is the FLIR ThermaCAM SC3000 that has a thermal sensitivity of 20 mK at 30 °C, an accuracy of 1% or 1°C for temperatures up to 150 °C. The GaAs, Quantum Well Infrared Photon FPA detector has a spectral range of 8–9 μm centred in one of the two atmospheric ''windows'' with a resolution of 320 x 240 pixels and is Stirling cooled to 70 K. The spatial resolution of the present camera is 31.25 μm for a focal distance of 26 mm. More detailed information about the IR measurements can be found in Buffone and Sefiane [13]. It is important to point out that the acetone used in this study is semi-transparent to IR at wavelengths of 8 to 9μm. The emissivity of acetone depends on the liquid thickness for drops (Brutin et al. [14]). Therefore, the IR measurements of the present investigation give an indication of the temperature distribution of the liquid close to the meniscus interface but not of the interface itself. However, the temperature oscillation frequency, as shown in Figure 3, is more important than an accurate measurement of the interface temperature and therefore the error made in the temperature measurement can be accepted. The present experiment was repeated 5 times using different tubes. We have estimated the change in temperature oscillations to be less than 0.2 °C which is close to the accuracy of the infrared camera of 0.1-0.14 °C in the range of the measured meniscus temperatures.

Figure 2. Temperature maps of meniscus interface at the capillary tube mouth during a standing wave. The two white circles indicate the capillary internal and external walls and the dashed lines in the second and third frame indicates the region of interest for the standing wave.

In Figure 3, we show the temperature evolution of five markers ("UP", "DOWN", "LEFT", "RIGHT" and "MIDDLE") over 20 s of IR recording. From Figure 3 it is clear that the unveiled hydrothermal wave is a standing wave rather than a travelling one, similar to the hydrothermal wave reported in Schwabe [10] and contrary to the travelling waves found in evaporating sessile drops [11]. Clearly "UP", "LEFT" and "MIDDLE" exhibit important temperature oscillations up to around 1.4°C, whereas "DOWN" and "RIGHT" do not seem to be affected in the same way by the standing wave; this is thought to be due to the fact that in the upper part of the meniscus, gravity and surface tension act in opposition, whereas in the lower part they act in the same direction. We have repeated the same experiment several times, also using two operators to understand why there is asymmetry between "LEFT" and "RIGHT" but we found similar results to those in Figure 3. The three-dimensional nature of the phenomenon and as such the slight imperfection in the flow could be amplified. The asymmetry is a kind of instability that is affected by minute instabilities in the temperature field at the meniscus interface. In order to capture this three-dimensional behaviour, more detailed studies - both experimental and numerical - are required. It is also worth noting that the standing wave seems to have some characteristic frequencies which are reported in Figure 4 where the power spectrum of the FFT of the temperature profiles in Figure 3 has been performed. There are three main frequencies around 0.3, 0.6, and 0.8 Hz.

Figure 3. Temperature evolution of five markers around the meniscus interface as indicated in the legend.

Figure 4. FFT of temperature evolution of five markers of Figure 3.

Figure 5 shows the temperature profiles along different lines in the tube cross-section "BEFORE" and "AFTER" the standing wave. As seen from the temperature plots of Figure 5, the 1% accuracy of the camera results in less than 0.15 °C accuracy at the maximum temperature of around 14 °C read along the meniscus interface. As this measures a temperature difference between "AFTER" and "BEFORE" the wave of over 1 °C, we can reasonably assume that with the camera used (with sensitivity of 20 mK) we can detect the temperature jump during the standing wave. The first thing worth noticing is the large temperature troughs at the meniscus contact line inside the capillary tube which are more than 12 °C less than ambient. This result confirms the findings of a previous work (Buffone and Sefiane [13]). The second important feature is the difference between left and right troughs in the profile at 0 rad compared to a much more even profile at $\pi/2$ rad; this is due to the fact, also argued in Buffone and Sefiane [13], that the single vortex present in the vertical section of the capillary tube brings hot liquid from the bulk in the upper part of the meniscus and heats up the contact line. The third and more interesting result for the present investigation is that there is a substantial variation of temperature before and after the standing wave and this variation is more marked for the upper region of the capillary tube cross-section.

Figure 5. Temperature profiles along indicated lines on the tube cross section "BEFORE" and "AFTER" the standing wave.

We have reported in Minetti and Buffone [15] that a dimensionless analysis involving the Marangoni number (Ma=$[(\partial\sigma/\partial T)(\partial T/\partial R)R^2]/\mu k$) and the Rayleigh numbers (Ra= $(g\beta\Delta T R^3)/\nu\, k$) along with their ratio, the Bond number (Bo=$(\rho g R^2)/\sigma$) indicates that for a 1 mm internal tube diameter, the estimated Bond number for the present case is less than 0.5. Here μ and ν are dynamic and kinematic viscosity and κ is thermal diffusivity. This confirms that, despite the fact the phenomenon is essentially Marangoni-driven, buoyancy effects are important and the competition between buoyancy and surface tension might well be responsible for the reported standing wave. Following the same analysis reported in Minetti and Buffone [15], assuming that the heat to sustain the evaporation comes from the surrounding environment, one can write:

$$m\ h_{fg} = 2\,\pi\, R\, k_a \left\{ 0.6 + \frac{0.387[C\ R^3\,(T_a - T_w)\ ]^{1/6}}{\left[1 + \left(\frac{0.559}{Pr}\right)^{9/16}\right]^{8/27}} \right\}^2 (T_a - T_w)$$

where m is the mass flux, h_{fg} is the latent heat of evaporation, k_a is the thermal conductivity of air, C is a constant incorporating air properties, T_a is the ambient temperature, T_w is the tube wall temperature, and Pr is the Prandtl number. Following the dimensional analysis derivation reported in Riley [16], we can define the Reynolds number as:

$$Re = \frac{Ma}{Pr} = \frac{U\, R}{\nu}$$

where U is the fluid velocity, R is tube radius and ν the kinematic viscosity. From this latter equation the fluid characteristic velocity can be written as (Riley [16]):

$$U = \frac{\frac{\partial\sigma}{\partial T}\frac{\partial T}{\partial R}R}{\mu}$$

from which the characteristic frequency (f^*) is the reciprocal of the convection time scale (τ) and can be written as (Buffone et al. [4]):

$$f^* = \frac{1}{\tau} = \frac{\frac{\partial\sigma}{\partial T}\frac{\partial T}{\partial R}}{\mu}$$

Now, we can assume with reasonable accuracy that the temperature oscillations cause the flow oscillations and the two frequencies are very similar (Buffone et al. [5]). Therefore, f^* is also a proxy of meniscus surface temperature oscillations. If we calculate f^* and the Marangoni number for acetone and compare it with the measurements done recently using ethanol [17], one gets the values reported in the following Table (Table 1) from which it can clearly be seen that acetone generates more vigorous instabilities and convection than ethanol; this is because acetone is much more volatile. On Table 1 the temperature gradient is calculated taking the readings between wedge and centre of the meniscus.

Table 1. Liquids properties and calculated Marangoni number and characteristic frequency (f*).

Liquid	Density	Surface Tension	Surface tension derivate	Specific heat	Kinematic viscosity	Dynamic viscosity	Thermal conductivity	$\frac{\partial T}{\partial R}$	Marangoni Number	Characteristic Frequency
	Kg/m^3	N/m	N/m/K	J/Kg/K	m^2/s	Pa s	W/m/K	K/m		Hz
Ethanol	792	0.023	9.65 x 10^{-5}	2372	1.6 x 10^{-6}	1.27 x 10^{-3}	0.17	9.87	1598	0.75
Acetone	799	0.025	1.25 x 10^{-4}	2112	4.4 x 10^{-7}	3.50 x 10^{-4}	0.16	12.9	8475	4.61

REFERENCES

[1] V. G. Levich and V. S. Krylov, Surface tension driven phenomena, Annu. Rev. Fluid Mech. 1, 293 (1969).

[2] J. R. A. Pearson, On convection cells induced by surface tension, J. Fluid Mech. 4, 489–500 (1958).

[3] L.E. Scriven, C. V. Sternling, The Marangoni effects, The Marangoni effects, Nature 187: 186–188 (1960).

[4] C. Buffone, K. Sefiane and J. R. Christy, Experimental investigation of self-induced thermocapillary convection for an evaporating meniscus in capillary tubes using micro-PIV, Physics of Fluids 17, 052104 (2005).

[5] C. Buffone, K. Sefiane and W. Easson, Marangoni-driven instabilities of an evaporating liquid-vapor interface, Physical Review E 71, 056302 (2005).

[6] M. K. Smith, S. H. Davis, Instabilities of dynamic thermocapillary liquid layers. Part 1. Convective instabilities J. Fluid Mech. 1983, 132, 119– 144

[7] S. H. Davis, Thermocapillary instabilities, Annu. Rev. Fluid Mech. 1987, 19, 403

[8] R. J. Riley and G. P. Neitzel, Instability of thermocapillary–buoyancy convection in shallow layers. Part 1. Characterization of steady and oscillatory instabilities, J. Fluid Mech. 1998,359, 143

[9] N. Garnier and A. Chiffaudel, Two dimensional hydrothermal waves in an extended cylindrical vessel, Eur. Phys. J. B 2001, 19, 87

[10] D. Schwabe, A. Zebib and B. C. Sim, Oscillatory thermocapillary convection in open cylindrical annuli. Part 1. Experiments under microgravity, J. Fluid Mech. 2003, 491, 239

[11] K. Sefiane, J. R. Moffat, O. K. Matar and R. V. Craster, Self-excited hydrothermal waves in evaporating sessile drops, Appl. Phys. Lett. 2008, 93, 074103

[12] D. Schwabe, Standing waves of oscillatory thermocapillary convection in floating zones under microgravity observed in the experiment MAUS G141, Adv. Space Res. Vol. 29, No. 4, pp. 651-660 (2002).

[13] C. Buffone and K. Sefiane, IR measurements of interfacial temperature during phase change in a confined environment, Experimental Thermal and Fluid Science 29, 65-74 (2004).

[14] D. Brutin, B. Sobac, F. Rigollet and C. Le Niliot, Infrared visualization of thermal motion inside a sessile drop deposited onto a heated surface, Experimental Thermal and Fluid Science 35: 521–530 (2011).

[15] C. Minetti and C. Buffone, Three-dimensional Marangoni cell in self-induced evaporating cooling unveiled by Digital Holographic Microscopy, Physical Review E 89, 013007 (2014).

[16] R. J. Riley, An investigation of the stability and control of a combined thermocapillary-buoyancy driven flow, Ph.D. dissertation, Georgia Institute of Technology, 1996.
[17] C. Buffone, K. Sefiane and C. Minetti, The effect of wall thickness and material on Marangoni driven convection in capillaries, Colloids and Surfaces A: Physicochem. Eng. Aspects 481 (2015) 384–392.

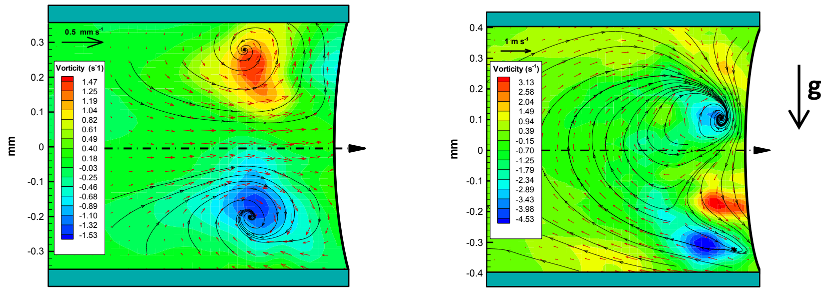
0.5 mm s-1
Vorticity (s-1)
1.47
1.25
1.19
1.04
0.82
0.61
0.49
0.40
0.18
-0.03
-0.25
-0.46
-0.68
-0.89
-1.10
-1.32
-1.53
mm
1 m s-1
Vorticity (s-1)
3.13
2.58
2.04
1.49
0.94
0.39
-0.15
-0.70
-1.25
-1.79
-2.34
-2.89
-3.43
-3.98
-4.53
g

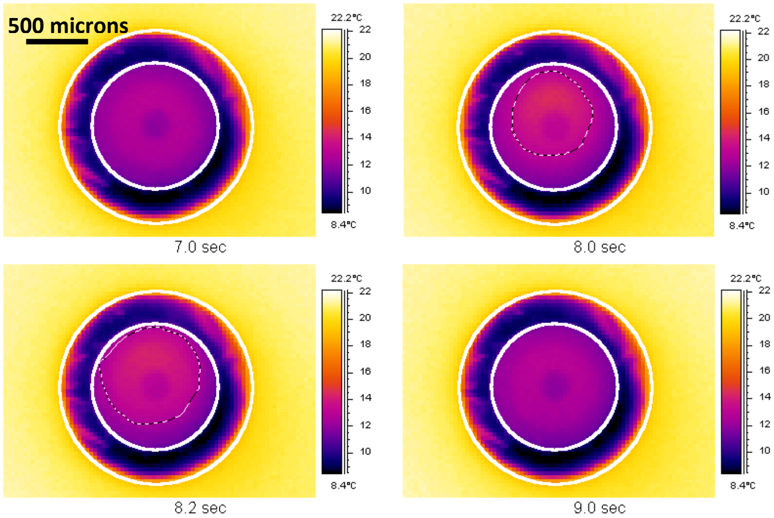
500 microns
7.0 sec
8.0 sec
8.2 sec
9.0 sec
22.2°C
8.4°C

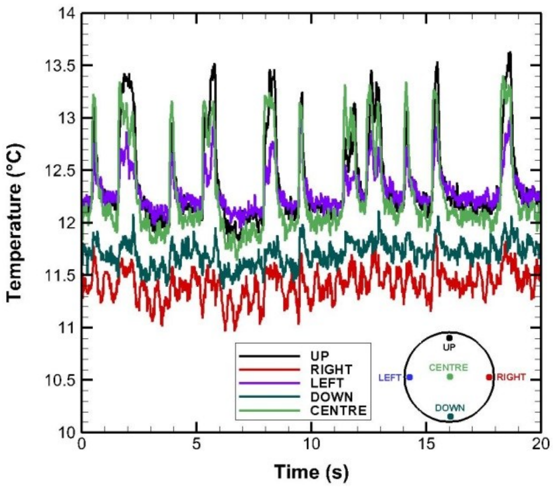
Temperature (°C)
Time (s)
UP
RIGHT
LEFT
DOWN
CENTRE

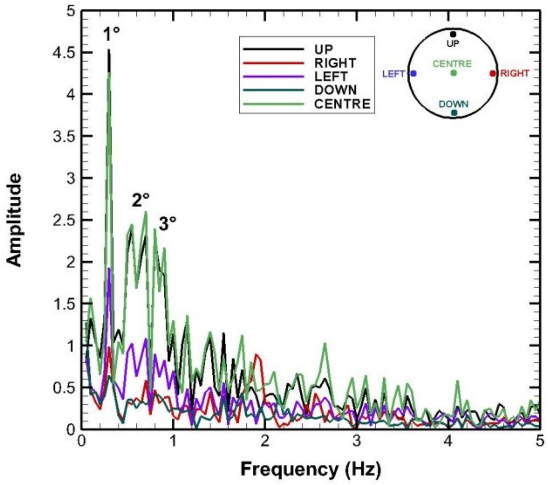

1°
2°
3°
UP
RIGHT
LEFT
DOWN
CENTRE
UP
CENTRE
LEFT
RIGHT
DOWN
Amplitude
Frequency (Hz)

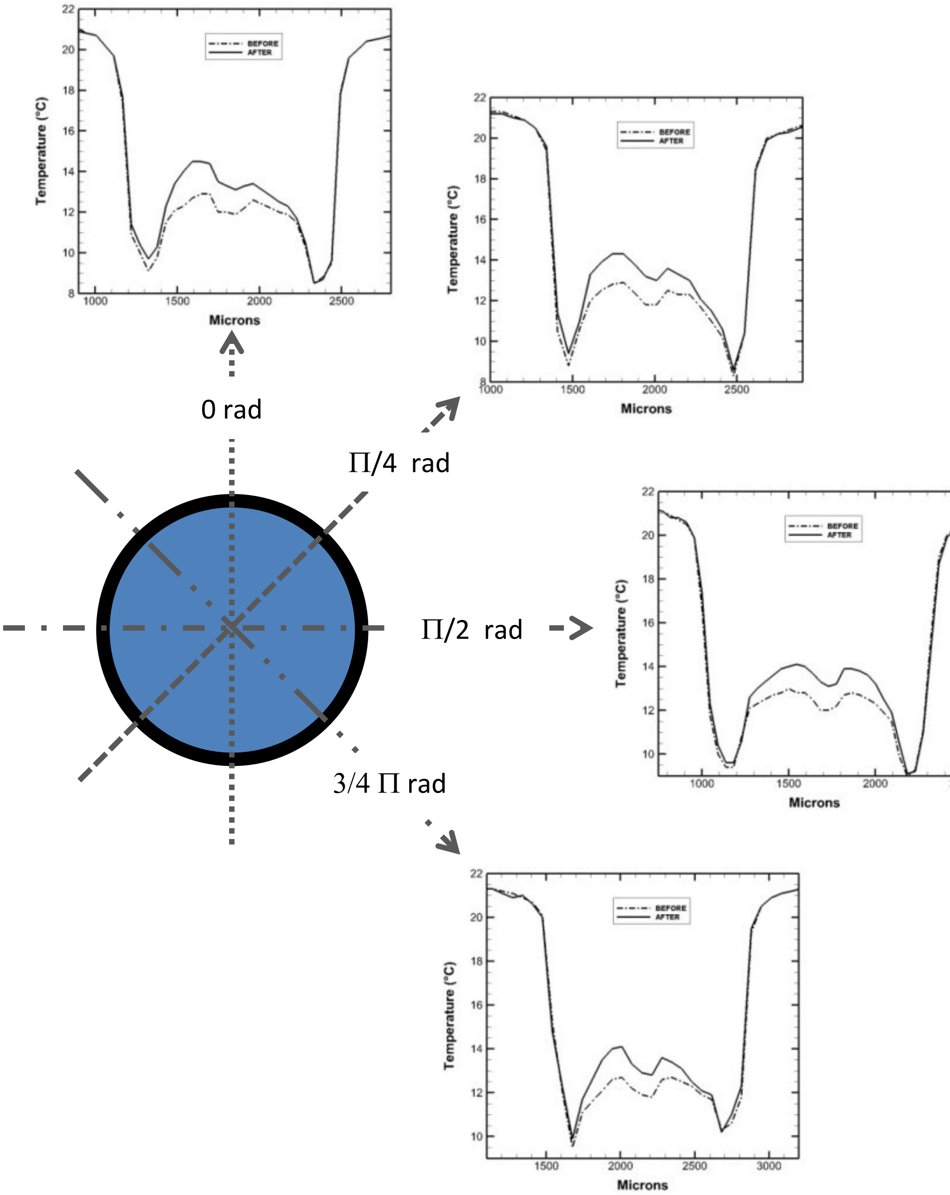
0 rad
Π/4 rad
Π/2 rad
3/4 Π rad
Temperature (°C)
Microns
BEFORE
AFTER